

A First-Principles Study of Aluminum-Polyethylene Interfaces

Lihua Chen*, Tran Doan Huan*, Ahmed Huzayyin†, Yenny Cardona Quintero* and Rampi Ramprasad*

*Institute of Material Science,
University of Connecticut,

97 North Eagleville Road Storrs, CT, 06269, USA

†Dept of Electrical and Computer Engineering,
University of Toronto,

10 Kings College Road Toronto, ON M5S 3G4, Canada

Abstract—The ideal interfaces of aluminum with different configurations of polyethylene were studied through first principles calculations based on density functional theory. The theoretical vacuum energy shift caused by interfacial dipole moments agrees well with experimental result for Al-tetratetracontane (TTC, $n\text{-CH}_3(\text{CH}_2)_{42}\text{CH}_3$) interface. Although the interfacial dipole moments are considered, the calculated charge injection barriers are still higher than the experimental barriers. The reason is likely that chemical defects exist at the interface but are not included in this work.

Keywords—Aluminum-polyethylene Interfaces, vacuum energy shift, charge injection barriers, first principles theory.

I. INTRODUCTION

Metal-polymer interfaces are important ingredients of a wide range of multilayer-structured electrical and electronic devices such as capacitors and electric cables. The performance of these devices is greatly shaped by a variety of interfacial phenomena [1], [2]. In particular, the physical and chemical processes of charge injection at the interface are believed to play a key role in the degradation and failure of the polymeric insulators in electronic devices.

Polyethylene (PE) is a typical polymer that has been widely examined in theoretical and experimental studies of the metal-polymer interfaces [3]–[5]. In spite of extensive efforts, the metal-PE interface is not yet fully understood. One of the reasons is that device level models do not capture the complex morphology of real PE samples, particularly at a molecular level [6], [7]. Charge injection barriers at the metal-PE interface are directly affected by a dipole layer which may be formed at the interface, due to chemical reaction and charge transfer. Previously, the calculated charge injection barrier based on the Schottky-Mott rule [8], [9] for idealized interfaces between metal and polymers, especially PE, are too high compared to the experimentally measured data [5], [10], [11]. The inconsistency suggests that interfacial dipole moments may play an important role in determining charge injection barriers [12].

The dipole moments formed at the interface induce the vacuum energy shift ($\Delta\varphi$), which affects the charge injection barriers (electron barrier ϕ_e and hole barrier ϕ_h), as illustrated in Fig. 1. The charge injection barriers depend on the band gap (E_g) and electron affinity (EA) of PE. These quantities may be computed using density functional theory (DFT) calculations.

However, the widely used exchange correlation potentials with in the local density approximation (LDA) and generalized gradient approximation (GGA) of DFT tend to underestimate band gap E_g of insulators by as much as 30% or more. The recently developed Heyd-Scuseria-Ernzerhof (HSE) hybrid functional [13] and many-body perturbation theory (GW) [14] are thus employed in the present work to determine the electronic properties of the Al-PE interface.

Practically, high adhesion is desired for metal-polymer interfaces [15]. Various methods were developed towards this goal, e.g., increasing the oxidation of polyethylene [16], [17] using copper clusters as “nano-nails” to anchor the deposited metals [18], and plasma modification of polymers [19], making the interfacial structure more complicated. Theoretically, the charge-injection barriers have not been well studied so far, because such concept can only be rigorously understood through a quantum mechanical description of the interface bonding. The above points suggest that a first-principles study of the relevant properties of the metal-polymer interfaces is desirable.

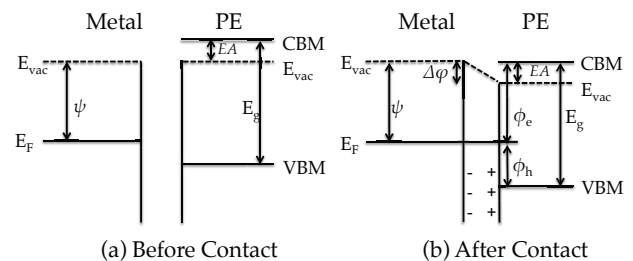


Fig. 1. Energy diagram of metal/PE (a) before contact and (b) after contact. E_F , E_{vac} , and ψ are Fermi level of the metal, vacuum energy level, and work function respectively. EA , CBM, VBM and E_g are electron affinity, conduction band minimum, valence band maximum and band gap of PE, respectively. $\Delta\varphi$, ϕ_e and ϕ_h are, respectively, vacuum energy shift, electron barrier, and hole barrier.

Motivated by these considerations, we present in this paper a first-principles study on Al-PE interfaces with different configurations of PE, to both represent various crystalline orientation of PE as well as aspects of the amorphous phase which both are expected to exist at the interface. Various characteristics of the Al-PE interfaces, i.e., geometries, electronic properties, vacuum energy shift and charge-injection barriers, are examined. We find that the calculated vacuum

energy shift of Al-PE (110) agrees with experimental result for Al-tetratetracontane (TTC, $n\text{-CH}_3(\text{CH}_2)_{42}\text{CH}_3$) interface. By properly considering the interfacial dipole moment, charge-injection barriers are calculated and compared with experimental values.

II. METHODS AND MODELS

The calculations were performed within the frame work of density functional theory (DFT) [20], [21] as implemented in the Vienna *ab initio* simulation package (VASP). We used the Perdew-Burke-Ernzerhof (PBE) [22] generalized gradient approximation (GGA) functional for the exchange-correlation energies and a plane wave energy cutoff of 400 eV for the basis set. A vacuum slab of 14–16 Å was used to suppress the interactions between the system and its periodic images. In order to correct the underestimation of band gap of PE, the Heyd-Scuseria-Ernzerhof (HSE06) hybrid functional [13] and many-body perturbation theory (G_0W_0) [14] were used. Dense Monkhorst-Pack \mathbf{k} -point meshes of $14 \times 14 \times 14$ and $4 \times 4 \times 10$ were used to sample the Brillouin zones of bulk Al and bulk PE. For the interface model, the \mathbf{k} -point mesh used was $4 \times 4 \times 1$. van der Waals interactions, known to be important in stabilizing polymers like PE, were included using non-local vdW-DF correlation functional. Atomic coordinates were relaxed until atomic forces are smaller than 0.01 eV/Å. Table I lists the optimized lattice parameters of the examined bulk Al and PE. Good agreement between the results of the present work and other DFT results as well as experimental data [23]–[25] was obtained. With PBE, HSE06 and G_0W_0 , the calculated electronic properties of bulk PE are listed in Table II. The band gap of PE calculated by PBE, HSE06 and G_0W_0 are within 24%, 7%, and 1% of experiment, respectively.

In our model, heterostructures were created by placing different configurations of PE slabs on Al (111) (hereinafter referred to as Al) slab, as illustrated in Fig.2. Based on the convergence tests for the work function, 9 atomic layers for Al slab were used. The commonly made assumption of a single interface with one Fermi level relative to the CBM and VBM of PE, overlooks the fact that various stable orientations of PE can occur at interface with metals leads to a varying charge injection barriers. Accordingly, four possible configurations of PE, including PE (110), PE (001) and PE (001)*, as representatives of the crystalline phase and PE (Lamellae) which occurs in the amorphous phase were used to model the morphologically complex structures of PE. The orientation of PE chains in PE (110) is parallel to the Al slab and normal to the paper as shown in Fig.2 (a), PE (Lamellae) is constructed by folding the PE chains as shown in Fig.2 (b). The chain direction of PE in Al-PE (001) is normal to the Al slab (Fig.2 (c)) while the angle between Al surface and the chain direction of PE in Al-PE (001)* is about 80 (degree) as shown in Fig.2 (d). For Al-PE (Lamella), Al-PE (001) and Al-PE (001)* structures, (1×1) PE slabs were strained along a and b directions to match the $(3 \times \sqrt{3})$ Al slab. In the case of Al-PE (110), since the b direction is the chain direction of PE, $(3 \times 2\sqrt{3})$ Al slab at b direction was strained 3 % to match the PE (110) slab.

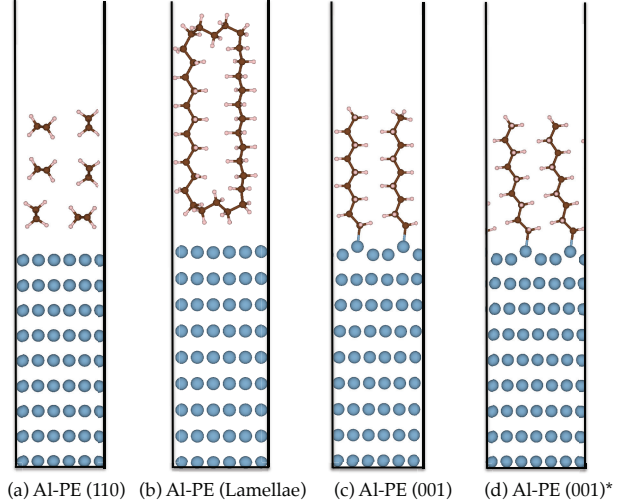


Fig. 2. Geometry of the examined Al-PE interface structures where Al, C, and H atoms are shown by blue, dark-brown, and pink spheres. (a) is Al-PE (110), whose PE chains parallel to Al plate and normal to the paper; (b) is Al-PE (Lamellae), in which PE chains are folded; the PE chains are both normal to Al surface for Al-PE (001), but the PE chains lean slightly for Al-PE (001)*.

TABLE I. OPTIMIZED LATTICE PARAMETERS OF PE AND THE BULK AL EXAMINED, GIVEN IN Å. FOR COMPARISON, DATA FROM EXPERIMENTAL AND OTHER DFT WORKS ARE ALSO GIVEN.

System	Lattice constants	This work	Other DFT	Experiments
PE	a	6.98	7.01 ^a	7.12 ^a
	b	4.78	4.76 ^a	4.85 ^a
	c	2.56	2.56 ^a	2.55 ^a
Al	a	4.05	4.06 ^b	4.05 ^c

^aRef. [23]; ^bRef. [24]; ^cRef. [25].

III. RESULTS AND DISCUSSIONS

A. Interfacial structure

Based on Fig.2, it is found that Al-C bonds (about 2 Å) are formed at Al-PE (001) and Al-PE (001)* interfaces due to the unsaturation of CH_2 at the beginning of PE chains. The bond angles (\angle_{AlCC}) of Al-PE (001) is larger (by 4 (degree)) than that of Al-PE (001)*. The effect of formation of Al-C bond on other properties is examined below. The interaction between Al and PE (110) and PE (Lamella) is probably a weak chemisorption/physisorption rather than chemical bonding.

B. Charge-injection barriers

According to the energy diagram presented in Fig.1, the charge injection barriers are defined as:

$$\phi_e = \psi - EA + \Delta\varphi, \quad (1)$$

$$\phi_h = E_g - \phi_e. \quad (2)$$

Here, ϕ_e , ϕ_h , ψ , EA , and $\Delta\varphi$ are, respectively, electron barrier, hole barrier, work function of Al, electron affinity of PE slab and vacuum energy shift. $\Delta\varphi$ is taken negative when the vacuum energy level of PE is decreased.

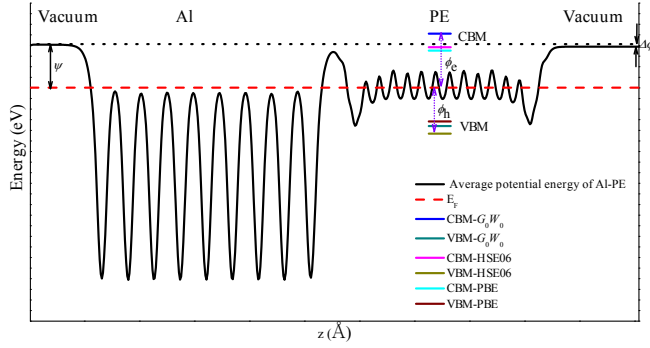


Fig. 3. Energy diagram of Al-PE interface with first-principles theory. Average potential energy of the Al-PE structure is black-solid curve. Work function ψ of Al is defined as the Fermi level E_F (red dash line) with respect to the vacuum level at Al side. The CBM and VBM of bulk PE with different computational methods are presented with blue, dark cyan, magenta, dark yellow, cyan and wine solid lines. The difference between vacuum energy level at PE side and CBM of PE is electron affinity EA . The $\Delta\varphi$ is the difference between the vacuum energy level at Al side and that at PE side, calculated with Eq. (3).

For the purpose of calculating the charge injection barriers, the work function ψ of Al, electron affinity EA of PE slab and vacuum energy shift were computed with the “Bulk plus band lineup” method [26], [27] firstly, as illustrated in Fig.3. We first calculated the planar average potential of different Al-PE slab and bulk structures of PE and Al. Then, the average potential of the bulk Al and PE structures are aligned with that of the model far from the surface to locate the relative position of E_F of Al and CBM of PE. The VBM position of PE is determined based on the CBM and E_g of PE. The computed work function ψ of normal and strained Al slab are 4.05 eV and 4.26 eV, respectively, agreeing well with the experimental value (4.26 eV) [28]. As shown in Table II, the EA determined by HSE06 and G_0W_0 are in better agreement with the negative EA of PE which is obtained experimentally as -0.5 ± 0.5 eV [30] than the EA calculated using PBE. In general, the computational results with G_0W_0 are found to be in best agreement with experimental data, compared with those of other computational methods. In addition, it is found that the electron affinity of different PE slabs is close and independent on the orientation of PE.

The vacuum energy shift $\Delta\varphi$ at Al-PE interface is given by

$$\Delta\varphi = -\frac{eD}{\epsilon_0 A}. \quad (3)$$

Here, D , ϵ_0 , e and A are interfacial dipole moment, vacuum permittivity, electron charge and the area of the Al-PE interface, respectively.

Results of $\Delta\varphi$ calculated with PBE and ϕ_e , ϕ_h computed with different methods are shown in Table III. Due to the similar interfacial structures and interaction of Al-PE (110) and Al-PE (Lamellae), in which no chemical bonding occurs between PE and Al and just a partial exchange of charge association with weak chemisorption/physisorption, the $\Delta\varphi$ of them are close (-0.20 eV and -0.19 eV). Because of the unavailability

TABLE II. THE CALCULATED ELECTRONIC PROPERTIES OF BULK PE AND EA OF PE SLAB WITH DIFFERENT THEORETICAL METHODS, GIVEN IN eV.

Method	E_g	VBM	CBM	Electron affinity (EA)		
				PE(110)	PE (001)	PE (Lamellae)
PBE	6.68	-2.53	4.15	0.59	0.74	0.67
HSE06	8.15	-3.38	4.77	-0.05	0.13	0.05
G_0W_0	8.72	-2.67	6.05	-1.33	-1.18	-1.23
Exp	8.80 ^a				-1.20~0 ^b	

^aRef. [29]; ^bRef. [30].

of experimental results of $\Delta\varphi$ for Al-PE interfaces, the experimental $\Delta\varphi$ of tetratetracontane (TTC, $n\text{-CH}_3(\text{CH}_2)_{42}\text{CH}_3$) absorbed on Al surface [31], whose interfacial structure is close to Al-PE (110), are used as a reference. The calculated $\Delta\varphi$ (-0.20 eV) of Al-PE (110) is close to the experimental result for TTC (-0.30 eV) [31], showing that the computational scheme used in this work is reasonable. However, the $\Delta\varphi$ of Al-PE (001) and Al-PE (001)* are positive, (0.29 eV and 0.24 eV, respectively). The $\Delta\varphi$ of Al-PE (001) and Al-PE (110) are opposite in sign, indicating that the mechanisms of dipole formation at Al-PE interfaces are different.

A dipole pointing to PE surface will facilitate extraction of electrons from PE which should be reflected as a decrease in vacuum level at PE side (negative $\Delta\varphi$) and vice versa if the dipole is pointing to the Al surface. On the one hand, the interfacial bonding in Al-PE (001) and Al-PE(001)* will involve the unsaturated carbon accepting electrons from Al, which is shown in the Fig.2 (c) and (d) reflected as shift of Al atoms towards PE. This shift of atoms and attraction of electron will create a depletion of electrons on the Al surface and an accumulation at the PE, thus a net positive charge at the surface and a net negative charge at PE, leading to the increase of vacuum energy level at PE side. On the other hand, a partial redistribution of charge between Al and PE (110) [or Al and PE (Lamella)] will mostly be governed by the difference of electron affinity of PE and that of Al. PE as a crystal has a negative electron affinity which means it wants to push electrons away from the crystal. Al has a positive electron affinity and would accept electrons partially. This means a region of accumulation of electrons at Al (negative charge) and a region of depletion of electrons at PE (positive charge), which will decrease the vacuum energy level at PE side.

The results of ϕ_e calculated with PBE and G_0W_0 differ by up to 2 eV while for ϕ_h , the PBE results are smaller than the G_0W_0 result by 0.2 eV. These results show that the accuracy of the electronic structure strongly affects the accuracy of the charge injection barrier. The error in the PBE band gap is more reflected on the electron injection barrier than the hole injection one. For Al-PE interfaces, the experimental value of ϕ_e is 2.14 eV [3], significantly lower than both PBE and G_0W_0 results. Possible reason could be that the PE slab of our model was designed from PE that is free from chemical impurities such as carbonyl. Carbonyl impurities and Al surface defects exist at the interface but are not included in the model. Extra interfacial states created in the forbidden gap of PE by carbonyl impurities can reduce the barrier to charge injection. In addition, the interfacial dipole moments are influenced by the interfacial states, thus the vacuum energy shift is changed. The effect of carbonyl and other impurities and surface defects at the interface will be studied in the future.

TABLE III. VACUUM ENERGY SHIFT $\Delta\phi$ CALCULATED WITH PBE AND CHARGE INJECTION ϕ_e AND ϕ_h , DETERMINED WITH PBE, HSE06 AND G_0W_0 . UNIT: (eV)

System	$\Delta\phi$	ϕ_e			ϕ_h		
		PBE	HSE06	G_0W_0	PBE	HSE06	G_0W_0
Al-PE (110)	-0.20	3.47	4.11	5.39	3.21	4.04	3.33
Al-PE (Lamellae)	-0.19	3.18	3.80	5.08	3.50	4.35	3.64
Al-PE (001)	0.29	3.60	4.21	5.52	3.08	3.94	3.20
Al-PE (001)*	0.24	3.55	4.16	5.47	3.13	3.99	3.25

IV. CONCLUSIONS

We have studied the interfaces of Al-PE with first-principles theory. The band gap of bulk PE and the electron affinity of PE slab computed using many-body perturbation theory (G_0W_0) are found to be in best agreement with experimental results. The vacuum energy shift caused by interfacial dipole moment is discussed and the result (-0.20 eV) of Al-PE (110) agrees well with experimental result (-0.30 eV) for Al-tetratetracontane (TTC, $n\text{-CH}_3(\text{CH}_2)_{42}\text{CH}_3$) interface. However, the computed charge injection barriers are still higher than the experimental barriers, probably because chemical defects at interface (which exist in reality) are not included in our models.

V. ACKNOWLEDGEMENTS

This paper is based upon work supported by a Multidisciplinary University Research Initiative (MURI) grant from the Office of Naval Research. Computational support is provided by National Energy Research Scientific Computing Center.

REFERENCES

- [1] F. Faupel, T. Strunskus, M. Kiene, A. Thrun, and C. Bechtolsheim, "Metal-polymer interfaces," in *Proceedings of the 1998 IEEE International Conference on Solid-State and Integrated Circuit Technology*, Beijing, China, 1998, p. 206.
- [2] T. Mizutani, "Behavior of charge carriers near metal/polymer interface," in *Proceedings of the 2005 International Symposium on Electrical Insulating Materials*. Japan: IEEE, 2005, pp. 1–6.
- [3] D. M. Taylor and T. J. Lewis, "Electrical conduction in polyethylene terephthalate and polyethylene films," *J. Phys. D: Appl. Phys.*, vol. 4, p. 1346, 1971.
- [4] M. Taleb, G. Teyssedre, S. Roy, and C. Laurent, "Modeling of charge injection and extraction in a metal/polymer interface through an exponential distribution of surface states," *IEEE Trans. Dielectr. Electr. Insul.*, vol. 20, no. 1, pp. 311–320, 2013.
- [5] A. Huzayyin, S. Boggs, and R. Ramprasad, "Quantum mechanical study of charge injection at the interface of polyethylene and platinum," in *IEEE Conference on Electrical Insulation and Dielectric Phenomena*, Cancun, 2011, pp. 800–803.
- [6] U. Gedde and A. Mattozzi, "Polyethylene morphology," in *Long Term Properties of Polyolefins*, ser. Advances in Polymer Science, A.-C. Albertsson, Ed. Berlin: Springer, 2004, vol. 169, pp. 29–74.
- [7] T. Furukawa, H. Sato, Y. Kita, K. Matsukawa, H. Yamaguchi, S. Ochiai, H. W. Siesler, and Y. Ozaki, "Molecular structure, crystallinity and morphology of polyethylene/polypropylene blends studied by raman mapping, scanning electron microscopy, wide angle x-ray diffraction, and differential scanning calorimetry," *Polymer*, vol. 38, p. 1127, 2006.
- [8] W. Schottky, "Deviations from ohm's law in semiconductors," *Phys. Z.*, vol. 41, 1940.
- [9] W. G. J. H. M. Van Sark, L. Korte, and F. Roca, *Physics and technology of amorphous-crystalline heterostructure silicon solar cells*. Berlin: Springer, 2011.
- [10] G. Teyssedre and C. Laurent, "Charge transport modeling in insulating polymers: From molecular to macroscopic scale," *IEEE Trans. Dielectr. Electr. Insul.*, vol. 12, pp. 857–875, 2005.

- [11] I. G. Hill, A. Rajagopal, A. Kahn, and Y. Hu, "Molecular level alignment at organic semiconductor-metal interfaces," *Appl. Phys. Lett.*, vol. 73, no. 5, pp. 662–664, 1998.
- [12] Y. Morikawa, H. Ishii, and K. Seki, "Theoretical study of n-alkane adsorption on metal surfaces," *Phys. Rev. B*, vol. 69, no. 4, p. 041403, 2004.
- [13] J. Heyd, G. E. Scuseria, and M. Ernzerhof, "Erratum: "hybrid functionals based on a screened coulomb potential" [j. chem. phys. 118, 8207 (2003)]," *J. Chem. Phys.*, vol. 124, no. 21, pp. 219906–219906, 2006.
- [14] L. Hedin, "New method for calculating the one-particle green's function with application to the electron-gas problem," *Phys. Rev.*, vol. 139, no. 3A, p. A796, 1965.
- [15] G. Grundmeier and M. Stratmann, "Adhesion and de-adhesion mechanisms at polymer/metal interfaces: Mechanistic understanding based on in situ studies of buried interfaces," *Annu. Rev. Mater. Res.*, vol. 35, no. 1, pp. 571–615, 2005.
- [16] F. Bockhoff, E. T. McDonel, and J. Rutzler, "Effects of oxidation on adhesion of polyethylene to metals," *Ind. Eng. Chem.*, vol. 50, no. 6, pp. 904–907, 1958.
- [17] J. Evans and D. Packham, "Adhesion of polyethylene to copper: Reactions between copper oxides and the polymer," *J. Adhesion*, vol. 9, no. 4, pp. 267–277, 1978.
- [18] M. Menezes, I. Robertson, and H. Birnbaum, "Novel technique to improve adhesion between metal/polymer interfaces," *MRS Proceedings*, vol. 445, 1 1996.
- [19] M. Horakova, P. Spatenka, J. Hladik, J. Hornik, J. Steidl, and A. Polachova, "Investigation of adhesion between metal and plasma-modified polyethylene," *Plasma Processes Polym.*, vol. 8, no. 10, pp. 983–988, 2011.
- [20] P. Hohenberg and W. Kohn, "Inhomogeneous electron gas," *Phys. Rev. B*, vol. 136, no. 3B, p. B864, 1964.
- [21] W. Kohn and L. J. Sham, "Self-consistent equations including exchange and correlation effects," *Phys. Rev.*, vol. 140, no. 4A, p. A1133, 1965.
- [22] J. P. Perdew, K. Burke, and M. Ernzerhof, "Generalized gradient approximation made simple," *Phys. Rev. Lett.*, vol. 77, no. 18, p. 3865, 1996.
- [23] C.-S. Liu, G. Pilania, C. C. Wang, and R. Ramprasad, "How critical are the van der waals interactions in polymer crystals?" *J. Phys. Chem. A*, vol. 116, no. 37, pp. 9347–9352, 2012.
- [24] N. E. Singh-Miller and N. Marzari, "Surface energies, work functions, and surface relaxations of low-index metallic surfaces from first principles," *Phys. Rev. B*, vol. 80, no. 23, p. 235407, 2009.
- [25] C. Kittel, *Introduction to Solid State Physics*, 8th ed. New York: Wiley, 11 2004.
- [26] C. G. Van de Walle and R. M. Martin, "Theoretical study of band offsets at semiconductor interfaces," *Phys. Rev. B*, vol. 35, pp. 8154–8165, May 1987.
- [27] R. Ramprasad, N. Shi, and C. Tang, "Modeling the physics and chemistry of interfaces in nanodielectrics," in *Dielectric Polymer Nanocomposites*. New York: Springer, 2010, pp. 133–161.
- [28] W. M. Haynes, *CRC handbook of chemistry and physics*. CRC press, 2012.
- [29] N. Ueno, K. Sugita, K. Seki, and H. Inokuchi, "Low-energy electron transmission and secondary-electron emission experiments on crystalline and molten long-chain alkanes," *Phys. Rev. B*, vol. 34, pp. 6386–6393, Nov 1986.
- [30] K. Less and E. Wilson, "Intrinsic photoconduction and photoemission in polyethylene," *J. Phys. C*, vol. 6, no. 21, p. 3110, 1973.
- [31] H. Ishii, K. Sugiyama, E. Ito, and K. Seki, "Energy level alignment and interfacial electronic structures at organic/metal and organic/organic interfaces," *Advanced Materials*, vol. 11, no. 8, pp. 605–625, 1999.